scientific reports

Check for updates

OPEN

Establishing a GMP-compliant manufacturing process and phase-appropriate analytics for early development of a FiCAR T-cell product with a novel CAR spacer

Annu Luostarinen[1]✉, Arja Vuorela[1], Erja Kerkelä[1], Mimmi Patrikoski[1], Annika Kotovuori[1], Jan Koski[2], Jonna Ahoniemi[3], Kaarina Lähteenmäki[3], Jenni Lehtisalo[4], Terhi Oja[4], Henrik Paavilainen[5], Anu Autio[5], Marie Nyman[5], Veera Nikoskelainen[6], Virginie Kergourlay[5], Endrit Elbasani[5], Bert van Veen[4], Anil Thotakura[5], Hector Monzo[7], Päivi M. Ojala[7], Matti Korhonen[1,2], Heidi Hongisto[1,8] & Anita Laitinen[1,8]

There is a growing demand for chimeric antigen receptor (CAR) -T cells for clinical trials. Consequently, new centers capable of manufacturing advanced therapy medicinal products (ATMPs) are needed. In this study, we established a good manufacturing practice -compliant manufacturing process and phase-appropriate analytics for a novel autologous CD19-targeted CAR T-cell product, 19-FiCART. We evaluated the stability of fresh, healthy donor-derived leukapheresis products (LPs), produced 19-FiCART using a 12-day semi-automated process with CD4/CD8-positive cell enrichment and lentiviral transduction, and evaluated the in vivo efficacy of 19-FiCART in a xenograft mouse lymphoma model. The optimal hold time and temperature to maintain LP stability were up to 73 h at 2–8 °C. The 19-FiCART manufacturing process consistently yielded more than 2×10^9 highly viable CAR+T cells, which is considered sufficient for a clinical product. The 19-FiCART products also demonstrated potent anti-tumor activity both in vitro and in vivo. This paper provides a detailed description of the manufacturing process and analytics for 19-FiCART and provides insights into the development of a release strategy for novel CAR T-cell products intended for early clinical studies. Additionally, we present data on LP stability, which has broader implications for the development of various immune cell-based ATMPs.

Keywords CAR T-cell, ATMP, Early development, Manufacturing, Analytical testing

Chimeric antigen receptor (CAR) -T-cell therapies have yielded remarkable results in the treatment of hematological malignancies. Several autologous CAR T-cell products have received marketing approvals from the US Food and Drug Administration (FDA)[1] and the European Medicines Agency (EMA)[2]. The success of CAR T-cells in hematological cancer treatment has inspired a growing number of clinical studies targeting cancer and autoimmune diseases using both autologous and allogeneic CAR Ts, as well as other genetically modified immune cells[3]. The rapid development of novel cell-based immunotherapies necessitates new centers capable of manufacturing these cell products in compliance with good manufacturing practice (GMP) standards and advanced therapy medicinal product (ATMP) regulations[1,2]. Regional ATMP competence centers, including those operating in blood, tissue, and cell establishments, can accelerate patient access to new treatments by providing infrastructure for ATMP manufacturing in close proximity to the patients[4,5].

[1]Advanced Cell Therapy Centre, Finnish Red Cross Blood Service, Härkälenkki 13, 01,730 Vantaa, Finland. [2]Research and Development, Finnish Red Cross Blood Service, Helsinki, Finland. [3]Quality Management, Finnish Red Cross Blood Service, Vantaa, Finland. [4]Pharmaceutical Sciences, Orion Corporation Orion Pharma, Turku, Finland. [5]Immuno-Oncology, Oncology Research, Orion Corporation, Turku, Finland. [6]Protein and Antibody Engineering, Medicine Design, Orion Corporation, Turku, Finland. [7]Translational Cancer Medicine Research Program, University of Helsinki, Helsinki, Finland. [8]Heidi Hongisto and Anita Laitinen These authors contributed equally to this work. ✉email: annu.luostarinen@bloodservice.fi

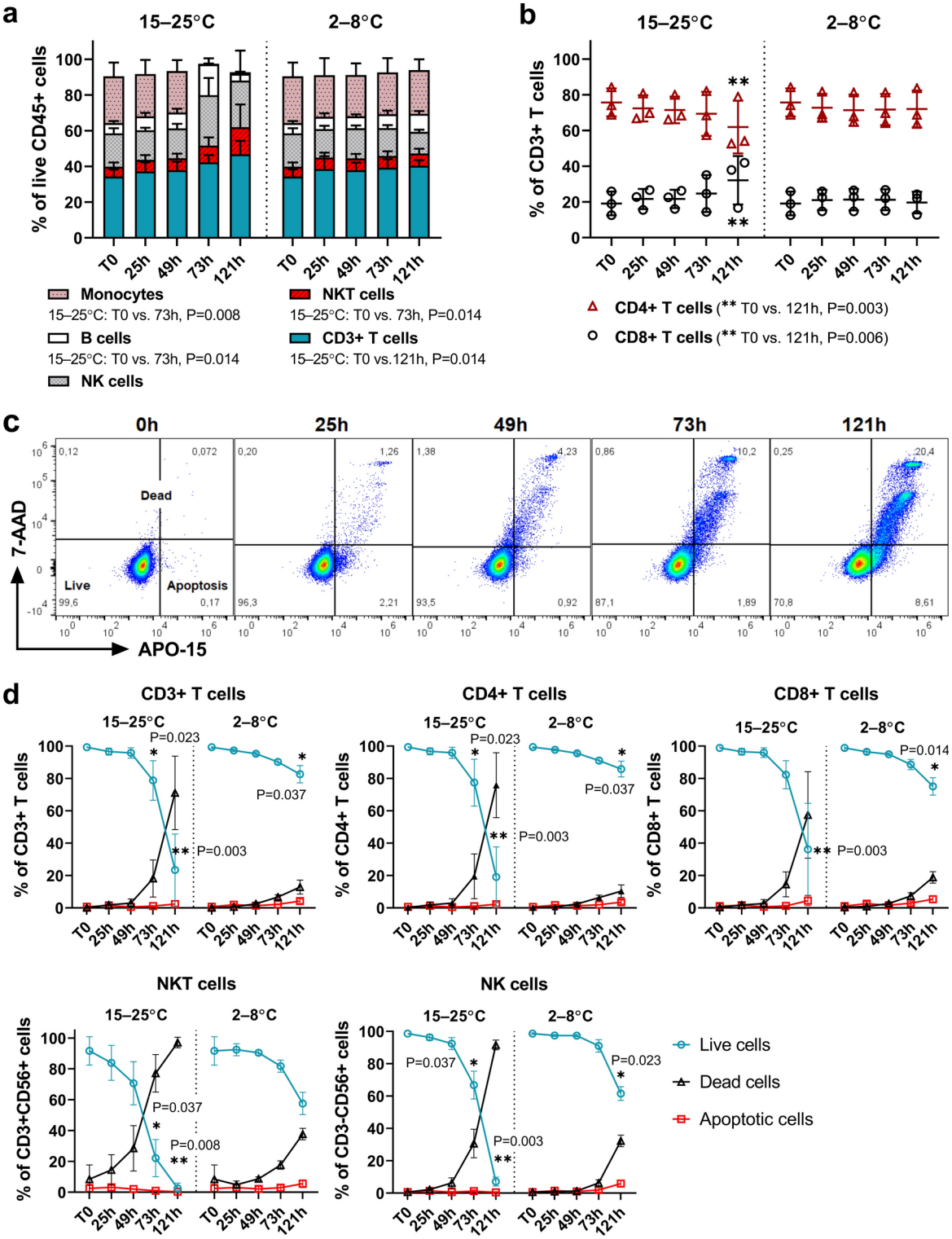

CAR T-cell manufacturing typically begins with leukapheresis to collect the patient's own leukocytes. T cells are then enriched from the leukapheresis product (LP) and modified to express CARs using lentiviral vectors (LVVs), retroviral vectors, or other methods[6]. Traditional manufacturing methods involve T-cell activation through CD3 and CD28 stimulation, followed by culturing for at least six days. However, the newest protocols prioritize shorter manufacturing times (less than two days) to achieve cost-efficient production and enhance clinical efficacy. These streamlined processes reduce vein-to-vein time and maintain high functional potency of minimally manipulated T cells[7].

In the centralized manufacturing model employed for current commercial CAR T-cell therapeutics, cryopreservation of the LP and the CAR T-cell product allows for extended transportation time between the clinic and the manufacturing site. This approach ensures completion of the quality control (QC) analytics for batch release before administering the product to the patient[8]. Alternatively, in a point-of-care manufacturing

◀**Fig. 1**. LP stability during a 121-h storage period at 15–25 °C and 2–8 °C. The frequencies of leukocyte subtypes, and cell-type specific viability and apoptosis were monitored at five timepoints (T0, 25 h, 49 h, 73 h, and 121 h) by FCM. **a**) Frequencies of monocytes, B cells, NK cells, NKT cells and CD3+ T cells within CD45+ leukocytes. **b**) Frequencies of CD4+ cells and CD8+ cells in the CD3+ T cell population. **c**) The FCM gating strategy utilized for the analysis of cell viability and apoptosis by 7-AAD and APO-15 shown for a representative LP sample stored at 2–8 °C. **d**) The proportions of live, dead, and apoptotic cells in CD3+ T cell, CD4+ T cell, CD8+ T cell, NKT cell, and NK cell populations. Data are shown as mean ± SD (n = 3, healthy donor-derived LPs). Statistical analysis of differences between the leukocyte subpopulation frequencies (**a**, **b**) and the percentage of live cells (**d**) at different time points by Friedman's nonparametric ANOVA followed by Dunn's post-test for multiple comparison for comparing the results at each timepoint with T0 (*P < 0.05, **P < 0.01). P-values are shown in the legend (**a**, **b**) or the figure (**d**). LP; leukapheresis product; FCM, flow cytometry; 7-AAD, 7-aminoactinomycin; APO-15, Apotracker Green.

model, fresh starting material is used to produce CAR T-cells directly within the hospital or a local center. This strategy simplifies logistics and enables patient treatment with freshly manufactured CAR T-cells. If a preliminary sterility test is used for batch release, QC tests can be partially completed after product administration[9].

Establishing GMP-compliant procedures for the manufacturing and QC of ATMPs is a complex endeavor. While commercially available platforms, such as the CliniMACS Prodigy (Miltenyi Biotec, hereinafter referred to as Prodigy) T-cell transduction (TCT) process[10], provide practical solutions for T-cell selection, transduction, and culture in a closed system. Despite using such platforms, manufacturers still need to address open process steps and QC independently. Careful definition of the product's critical quality attributes (CQAs), identification of sampling points, and selection of appropriate analytical methods are crucial to ensure the safety and functionality of the ATMP[11]. Product release testing should include the analysis of appearance, quantity, identity, purity, impurities (both product- and process-related), potency, and microbial safety[12]. Justifying the acceptance criteria based on manufacturing experience can be challenging, especially when dealing with a limited number of development batches due to high manufacturing costs. Only limited information on the QC strategies of commercial or investigational ATMPs is publicly available for reference to newcomers in the field.

We recently developed FiCAR, a CAR based on signal-regulatory protein α (SIRPα) spacer. FiCAR is designed to enhance CAR T-cell functionality by minimizing interactions with cells expressing the IgG's crystallizable fragment-binding receptor[13]. In the current work, we establish a GMP-compliant manufacturing process and phase-appropriate analytics for an autologous CD19-targeted CAR T-cell product (19-FiCART) intended for the treatment of adult patients with high-risk B-cell lymphoma. We assessed cellular starting material stability using LPs from healthy donors and set up a Prodigy TCT-based manufacturing process and analytical testing methods for in-process control and batch characterization of 19-FiCART. We also evaluated the in vivo efficacy of 19-FiCART in a xenograft lymphoma model. This paper describes the 19-FiCART manufacturing process and planned QC strategy and discusses appropriate batch release tests for early clinical studies.

Results

The cell composition and viability of cells in leukapheresis products remain stable for at least 25 h at room temperature and 73 h at cool temperature

We assessed the stability of fresh, healthy donor-derived LPs at room temperature (RT; 15–25 °C) and cool temperature (CT; 2–8 °C) during a 5-day follow-up period to define the optimal storage conditions and maximum hold time between apheresis and 19-FiCART manufacturing (Fig. 1). LP appearance remained unchanged at both temperatures until the latest timepoint (121 h), when the color of the products stored at RT was darker red compared to those stored at CT, potentially indicating accelerated red blood cell fragmentation at RT. Throughout the study, white blood cell (WBC) counts remained consistent at both temperatures (Supplementary Fig. S1A), indicating minimal leukocyte disintegration in the LPs.

At T0 (representing the analysis immediately after apheresis), the leukocytes in the LPs were composed of (mean ± SD) 26.1 ± 7.7% monocytes, 5.8 ± 1.1% B cells, 18.7 ± 2.8% NK cells, 5.5 ± 2.4% NKT cells and 34.3% ± 4.1% CD3+ T cells (Fig. 1a). The CD3+ T cell population encompassed 75.7 ± 7.8% CD4+ T cells and 19.1 ± 6.7% CD8+ T cells (Fig. 1b). The leukocyte composition remained stable throughout the 121-h follow-up at CT (Fig. 1a–b). In the RT-stored LPs, the frequency of monocytes decreased rapidly after the 49 h timepoint, being < 1% at 73 h (Fig. 1a). Similar collapses were not observed in other leukocyte subpopulations during RT-storage, but the frequencies of all the assessed cell types showed increasing variation starting from 73 h at RT, suggesting decreased stability. Statistically significant differences compared to T0 were detected in the frequencies of T cells, NKT cells, and B cells at 73 h or 121 h RT (Fig. 1a–b).

CD45+ leukocytes, CD3+, CD4+, and CD8+ T cells, and NK cells remained ≥ 90% viable until 73 h at CT and until 49 h at RT, after which their viability begun to deteriorate (Supplementary Fig. S1B and Fig. 1c–d). Monocytes and B cells maintained > 90% viability throughout the 5-day follow-up at CT but declined rapidly after 49 h at RT (Supplementary Fig. S1B). NKT cell viability was comparable to the viability of T and NK cells at CT but exhibited higher variation and faster decline at RT (Fig. 1d). Irrespective of the storage temperature, the average proportions of apoptotic cells in the products remained low throughout the study, though the products stored at RT contained somewhat fewer apoptotic cells than those stored at CT (Fig. 1d). At 121 h, the proportions of apoptotic cells, including all cell types, were 4.9% ± 2.0% at CT and 1.2% ± 1.6% at RT (Fig. 1d). Based on these results, LPs remained stable for at least 25 h at RT and 73 h at CT.

19-FiCART cells are efficiently transduced and expanded using a semi-automated process and the resulting cells demonstrate active in vitro anti-tumor functionality

We established a platform for the production and analytical testing of 19-FiCART. This platform includes a 12-day semi-automated manufacturing process with CD4/CD8-positive cell selection and lentiviral transduction, as well as phase-appropriate analytics for testing the LP starting material, in-process controls (IPCs), the harvested drug substance (DS), and the drug product (DP) in its final formulation (Fig. 2).

CD4/CD8-enrichment

Key data of the CD4/CD8-enrichment parameters, including the cell count, viability, frequency, total count, and recovery of CD4/CD8-labeled cells in the LPs and the enriched positive fractions are shown in Table 1. In 19-FiCART processes #1–3, about 60 mL of LP material was used for CD4/CD8-enrichment. The enrichment step yielded $1.07 \times 10^9 \pm 0.48 \times 10^9$ cells in the CD4/CD8-positive fraction with approximately 90% purity and 61% recovery of CD4/CD8-labeled cells (Table 1). Thus, the required 0.1×10^9 CD4/CD8-labeled cells for culture setup were successfully obtained in all three process runs.

Cell composition

The frequency of CD3+ T cells increased from an initial proportion of (mean ± SD) 35.2 ± 5.5% in the LPs to 79.3 ± 3.0% in the day (d)0 CD4/CD8-enrichment positive fractions (d0 IPCs), and further increased to 94 ± 1.3% in the d12 DS products (Fig. 3a and Supplementary Table S1). The frequencies of CD4+ and CD8+ cells in the CD3+ T-cell population were (mean ± SD) 74.7 ± 8.4% and 19.5 ± 6.3% in the LP; 78.7 ± 7.5% and 18.4 ± 5.7% in the d0 IPCs; and 63.6 ± 6.5% and 35.8 ± 6.5% in the d12 DS products, respectively (Fig. 3b), showing an increase of the CD8+ T cell population during culture. Thereby, the ratio of CD4+ and CD8+ T cells (CD4:CD8) decreased during culture from (mean ± SD) 4.7 ± 2.2 in the d0 IPC to 1.8 ± 0.5 in the DS products (Fig. 3c).

NKT cells were the most prominent cellular impurity in the DS products, being present at (mean ± SD) 5.1 ± 1.8% in the LPs, 10.0 ± 2.6% in d0 IPCs, and 5.2 ± 2.1% in the d12 DS products (Fig. 3a). Other non-target

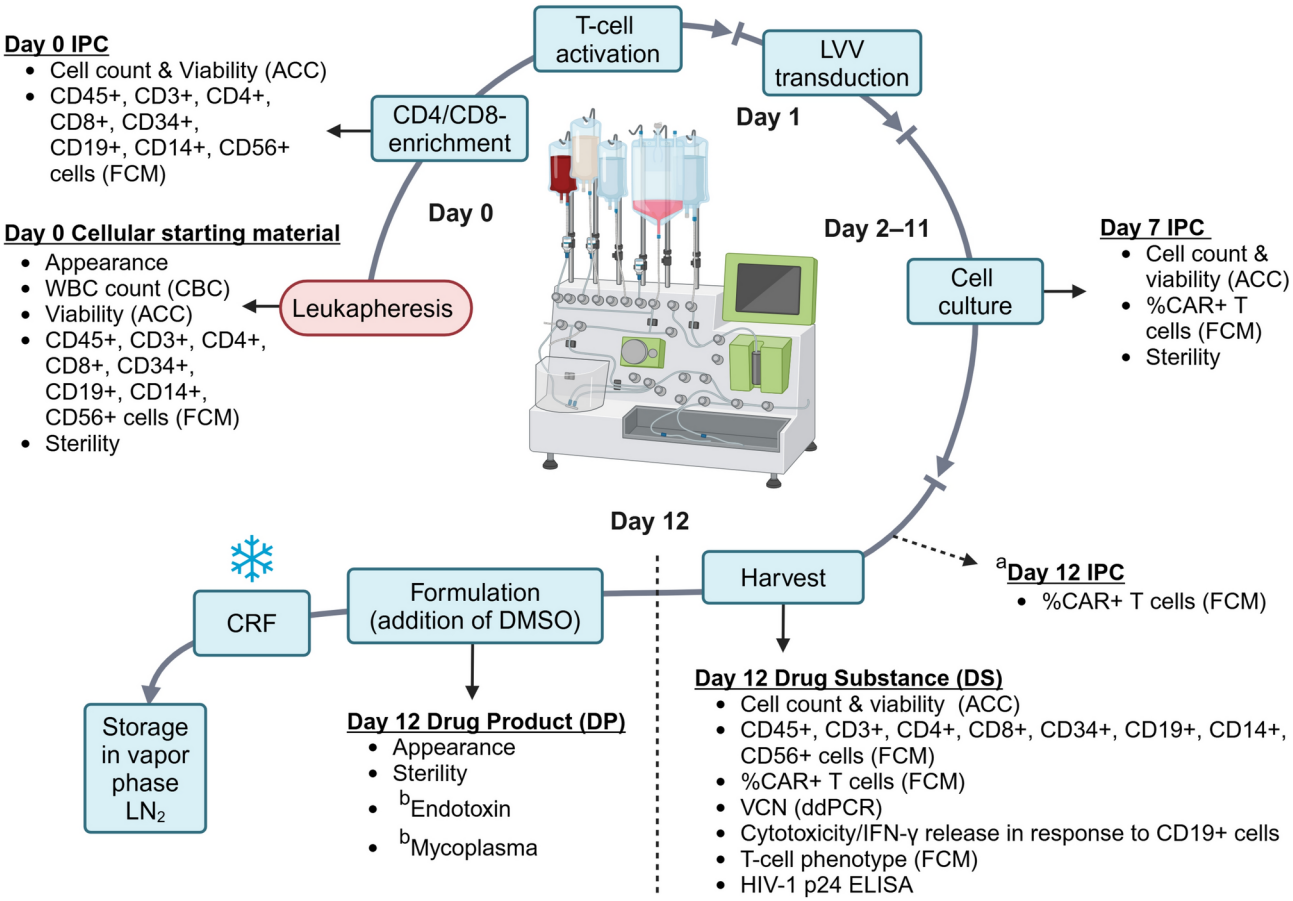

Fig. 2. Flow chart of the CliniMACS Prodigy-based manufacturing process and analytics conducted for the 19-FiCART batches #1–3. [a]Day 12 IPC was taken only for process #1. [b] Data are not available for endotoxin and mycoplasma tests. CBC, complete blood count; ACC, automated cell counter; IPC, in-process control; FCM, flow cytometry; LVV, lentiviral vector; VCN, vector copy number, ddPCR, droplet digital PCR; HIV-1, human immunodeficiency virus-1; CRF, controlled rate freezing; LN2, liquid nitrogen. Created in BioRender. Luostarinen, A. (2025) https://BioRender.com/i49l872.

Parameter	Leukapheresis product (starting material)		CD4/CD8-enrichment positive fraction	
	process #1; #2; #3	mean ± SD	process #1; #2; #3	mean ± SD
[a]Volume (mL)	62; 61; 57	60 ± 3	120; 80; 80	-
Cell count ($\times 10^6$/mL)	100.9; 60.1; 62.0	74.3 ± 23.0	14.5; 10.1; 12.6	12.4 ± 2.2
Viability (%)	99.4; 99.4; 98.8	99.2 ± 0.4	98.0; 98.9; 99.2	98.7 ± 0.6
CD4/CD8-cell frequency (%)	46.6; 31.9; 37.6	38.7 ± 7.4	92.3; 85.1; 90.2	89.2 ± 3.7
[a]CD4/CD8-cell total number ($\times 10^9$)	2.90; 1.17; 1.32	1.80 ± 0.96	1.61; 0.69; 0.91	1.07 ± 0.48
CD4/CD8-cell recovery (%)	-	-	55.4; 58.9; 68.8	61.0 ± 6.9

Table 1. CD4/CD8-cell count, viability, purity, total number, and recovery in the leukapheresis starting material and CD4/CD8-enrichment positive fraction. [a]The capacity of the CliniMACS Prodigy CD4/CD8-enrichment procedure is up to 10^9 CD4/CD8-labeled cells per enrichment stage. The enriched cells are eluted in 40 mL of culture medium per stage to the CD4/CD8-positive fraction. In process #1, 3 enrichment stages were performed, resulting in 120 mL, whereas processes #2 and #3 enrichments were performed using 2 stages, resulting in 80 mL volume of the CD4/CD8-positive fraction.

cells, including NK cells, monocytes, and B cells were effectively removed during the CD4/CD8-enrichment step and nearly or completely absent in the DS products (Fig. 3a and Supplementary Table S1). A small population of CD34+ cells (≤ 0.1%) was observed in the LPs but, importantly, not in the d0 IPCs and d12 DS products (Fig. 3d and Supplementary Table S1). Thus, the 19-FiCART DS products were composed of T cells and a minor proportion (< 7%) of NKT cells.

Transduction efficiency and vector copy number

To assess the relationship between the multiplicity of infection (MOI) used for transduction and the resulting transduction efficiency and vector copy number (VCN), we performed LVV transductions using HEK293T titer-based MOIs of 0.3, 0.8, and 1.5 in processes #1–3, respectively. In the resulting DS products (#1–3), CD3+ T cells contained 48.8%, 52.4%, and 78.5% CAR+ cells (Fig. 3e) and the VCN values were 1.20, 1.16, and 2.52 per cell (Fig. 3f), respectively. Thus, MOIs 0.3 and 0.8 yielded similar transduction rates, whereas an MOI of 1.5 clearly increased both the transduction efficiency and VCN. The frequency of CAR+ cells was approximately 20%, 10%, and 5% higher in CD4+ T cells than in CD8+ T cells in processes #1–3, respectively (Fig. 3e). The NKT cell populations in the DS products contained 23–33% CAR+ cells (Supplementary Fig. S2A).

The 19-FiCART QC plan (Fig. 2) involved analyzing transduction efficiency on d12 before (d12 IPC) and after harvest (DS). Notably, there were no discernible differences in lymphocyte compositions between d12 IPC and DS samples. This consistency held true for the frequency of CD3+ T cells, CD4+ T cells, CD8+ T cells, NK cells, and NKT cells (Supplementary Fig. S2B) as well as the percentage of CAR+ CD3+ , CD4+ , or CD8+ T cells (≤ 1% differences between d12 IPC and DS; Supplementary Fig. S2C). Thus, the d12 results of the FCM analyses performed before and after harvest were comparable.

Cell numbers and viability

Approximately 50-fold expansion efficiency of live cells was achieved in the three process runs (Fig. 3g). The total live cell number increased from the initial number of 10^8 activated CD4/CD8-enriched cells to 4.56×10^9, 4.66×10^9, 5.13×10^9 in the DS product in process #1–3, respectively (Fig. 3h). The total number of live CAR+ T cells in the DS product was 2.08×10^9, 2.33×10^9, and 3.74×10^9 in process #1–3, respectively (Fig. 3h). Cell viability was ≥ 96% throughout the manufacturing process in all three runs (Fig. 3i).

Vector-derived p24 protein impurity

We also quantified the amount of residual vector-derived Human immunodeficiency virus-1 (HIV-1) p24 protein impurity in the products using an ELISA assay. We detected residual p24 protein in the DS product supernatants of all three product batches, p24 concentrations being 6.1, 13.7, and 14.7 pg/mL for processes #1–3, respectively (Fig. 3j). The standard curve of the analytical kit starts from 12.5 pg/mL (range 12.5–200 pg/mL), rendering the value measured for process #1 interpretable as negative for p24. Overall, p24 was present in the DS supernatants at low or negligible concentrations.

T-cell phenotype

We conducted a comprehensive evaluation of the differentiation status of 19-FiCART cells by analyzing the T-cell memory subtypes and expression of T-cell exhaustion markers on CD4+ and CD8+ cells by FCM. CD95-negative naïve T cells were detected in the d0 IPCs (16–48% of CD4+ and CD8+ cells) but not in the d12 DS products, whereas the proportion of stem cell memory T cells (T_{SCM}) increased from an initial frequency of 1–3% in the d0 IPC CD4+ and CD8+ populations to 37–58% in the CD4+CAR+ and CD8+CAR + cells in the DS products, indicating that the culture conditions favored the generation of T_{SCM} cells (d0 data not available for process #1; Supplementary Fig. S3A).

The CAR+ cells in the DS products contained considerable proportions of less differentiated T_{SCM} and central memory (T_{CM}) cells (%T_{SCM} + %T_{CM}, min–max: 67–85% of CD4+CAR+ cells and 45–74% of CD8+CAR+ cells; Fig. 4a–b). In both CD4+ and CD8+ populations, but more apparently within CD8+ cells, CAR+ cells had

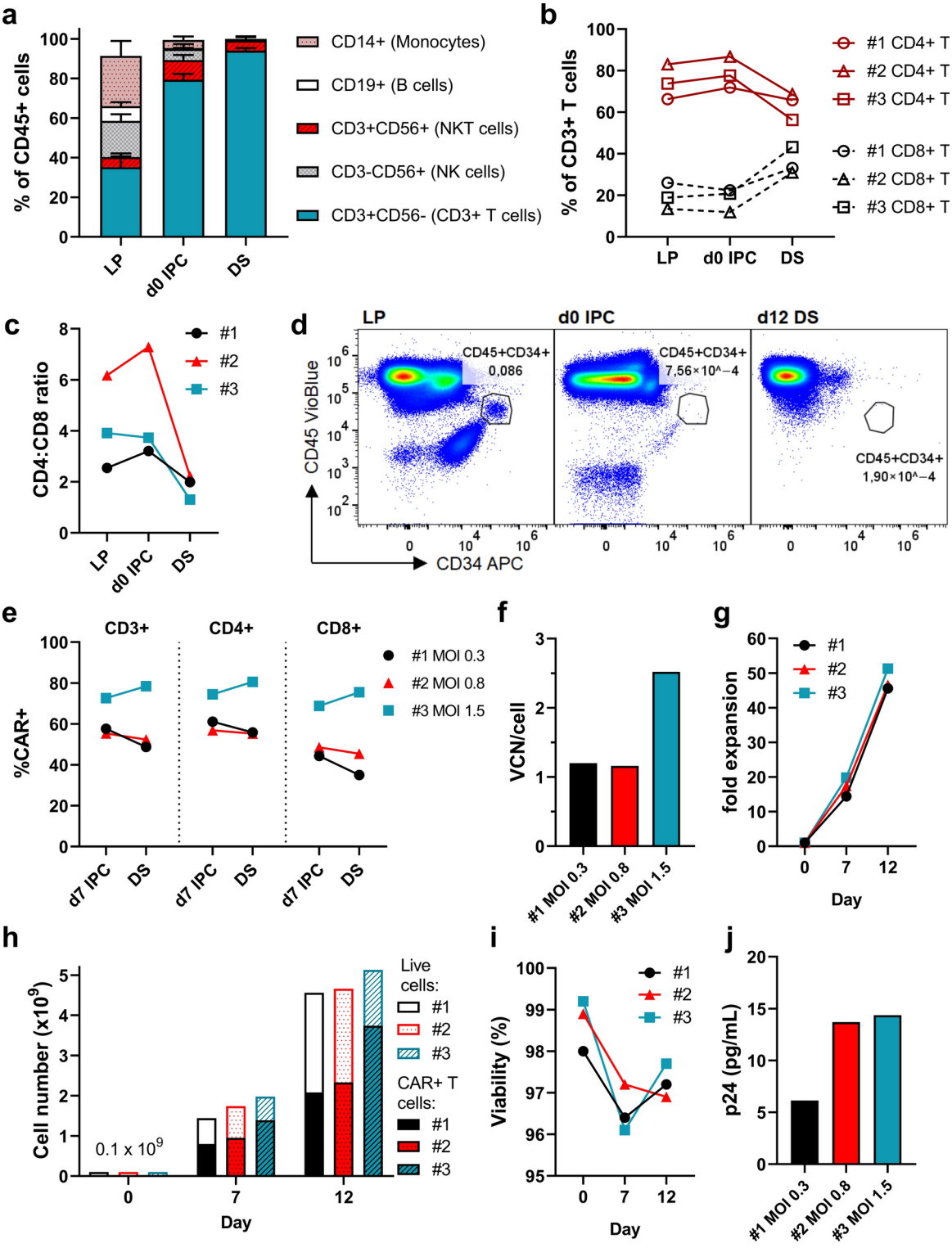

slightly less differentiated T-cell memory phenotype than CAR-negative cells, which was observed as somewhat higher frequency of T_{SCM} cells and smaller proportion of effector memory (T_{EM}) cells in CAR+ cells as compared to CAR-negative cells (Fig. 4a). Similarly, the frequencies of cells expressing T-cell exhaustion markers PD-1, LAG-3, and CD57, were slightly lower in CAR+ cells as compared to CAR-negative cells, statistically significant difference being detected for the frequencies of cells expressing PD-1 within CD4+ cells and CD57 within CD8+ cells (Fig. 4c; median fluorescence intensities are shown in Supplementary Fig. S3B).

The majority (>90%) of both CAR-negative and CAR-expressing CD4+ and CD8+ cells were positive for CD25 and Tim-3 (Fig. 4c), indicating proper T-cell activation by CD3/CD28 stimulation[14,15]. In the three process runs, (min–max) 0.4–6.5% of CAR+ cells in the CD4+ and CD8+ populations co-expressed PD-1 together with LAG-3, CD57, or Tim-3 (Fig. 4d), suggesting minimal exhaustion stage in the products.

◀**Fig. 3**. 19-FiCART product cell composition, transduction efficiency, and cell yield. **a**–**b**) Frequencies of CD3+ T cells, NK cells, NKT cells, monocytes, and B cells within live CD45+ cells (**a**), and frequencies of CD4+ T cells and CD8+ T cells within the CD3+ T cell population (**b**) in the LP, d0 IPC (CD4/CD8-enrichment positive fraction), and d12 DS measured by FCM. **c**) The ratio between CD4+ and CD8+ T cells in LP, d0 IPC, and d12 DS. **d**) Representative FCM plots showing the analysis of CD45dimCD34+ cells in LP, d0 IPC, and d12 DS (process #3). **e**) Frequency of CAR+ cells within CD3+ , CD4+ , and CD8+ T cells in measured in the middle (d7 IPC) and at the end of the process (d12 DS). **f**) Mean VCN per cell in d12 DS analyzed by droplet digital PCR. **g**–**h**) Fold expansion of live cells during culture (**g**), total count of live cells and CAR+ T cells (**h**), and percentage of live cells (**i**) on days 0, 7, and 12. **j**) Concentration of lentiviral p24 protein impurity in the d12 DS supernatant measured by ELISA. Data are shown as mean with SD of three process runs (**a**) or individually for the process runs #1–3 (**b**, **c**, **e**–**j**). LP, leukapheresis product; d, day; IPC, in-process control; DS, drug substance; FCM, flow cytometry; VCN, vector copy number.

In vitro cytotoxicity and interferon-γ secretion in response to CD19+ cells

We assessed the potency of 19-FiCART by measuring the in vitro cytotoxicity and interferon (IFN)-γ secretion of DS product cells in response to two CD19+ luciferase-expressing cell lines, NALM-6 and Raji (Fig. 4e–h). In the potency assays, the 19-FiCART cells were co-cultured with the target cell lines at different effector to target cell ratios (E:T) for 20 h. All three 19-FiCART cell batches demonstrated significantly higher cytotoxicity (Fig. 4e, g) and IFN-γ secretion activity (Fig. 4f, h) than non-transduced (NT) control cells produced from the same donor.

Considerations for 19-FiCART batch release criteria during early clinical development

The planned batch release criteria for early-phase development of 19-FiCART are presented together with results of production runs #1–3 in Table 2. The tests include analyses for appearance, purity (%CD3+ T cells), impurities (%CD19+ cells and %CD34+ cells), identity (%CAR+CD3+ T cells), potency (viability, %CAR+CD3+ T cells, and VCN), quantity (total number of viable CAR+CD3+ T cells), and safety (VCN, sterility, endotoxin, and mycoplasma). Microbial sterility test results were negative for all three production runs. Data are not available for the endotoxin and mycoplasma tests.

19-FiCART cells show a robust anti-tumor response in a Raji xenograft model

Having successfully established the manufacturing process and batch characterization tests for 19-FiCART, we evaluated the in vivo efficacy of 19-FiCART batch #3 cells against Raji cell lymphoma xenografts in NSG mice. Prior to the in vivo study, we confirmed that the cell composition and CAR expression of the thawed 19-FiCART batch #3 cells were comparable to d12 DS before cryopreservation (Supplementary Fig. S4A–B). Additionally, the thawed 19-FiCART cells showed active cytotoxicity against NALM-6 and Raji cell lines in vitro (Supplementary Fig. S4C–D). NSG mice xenografted with RedFluc-GFP-Raji cells received infusions of 5 M and 10 M 19-FiCART cells, 10 M NT cells, or PBS (Fig. 5a and Supplementary Fig. S5A). Remarkably, five-to-ten days after T-cell infusion, the 19-FiCART 5 M and 10 M mice groups showed a significant reduction in tumor burden (as depicted by the absence of bioluminescence signal) (Fig. 5b–c, Supplementary Fig. S5B–D, and Supplementary Table S2). The 19-FiCART-treated mice remained tumor-free throughout the study period (d60). The 10 M NT-treated mice showed progressive tumor load reduction 15-to-20 days after T-cell infusion, indicating a CAR-independent anti-tumor response, likely due to graft-*vs*-tumor effects[16,17] (Fig. 5b–c and Supplementary Fig. S5B–C). In contrast, the PBS-treated mice group showed continuous tumor growth. All PBS-treated mice displayed severe health deterioration in the form of hindlimb paralysis and weight loss (body condition score, BCS ≈ 1–2[18]) and had to be euthanized (d13–d17). All 10 M NT-treated mice, at a later phase of the experiment, six 10 M 19-FiCART-treated mice, and two 5 M 19-FiCART-treated mice presented signs of distress and health deterioration such as weight loss, lack of activity and hunched posture (BCS ≈ 1–2), and were euthanized (d34–d44 NT mice, and d42–d49 19-FiCART mice), typical symptoms of xenogeneic graft-vs-host disease (GvHD). The remaining two 10 M 19-FiCART-treated mice and six 5 M 19-FiCART-treated mice showed good health, activity, and behavior (BCS ≈ 3) until the end of study at d60 (Fig. 5d and Supplementary Fig. S6). These results suggest that the dose of ≈ 5×10^6 19-FiCART cells demonstrated effective anti-tumor efficacy in the Raji xenograft mouse model.

Discussion

In this study, we established a manufacturing process and phase-appropriate analytical tests for 19-FiCART, a novel autologous CD19-targeted CAR T-cell product intended for treating adult patients with high-risk B-cell lymphoma. We produced three process development batches of 19-FiCART using fresh LPs from healthy donors using a Prodigy-based manufacturing process and LVVs provided by a GMP-competent contract development and manufacturing organization (CDMO). In this section, we describe the 19-FiCART manufacturing process, outline the planned QC strategy, and discuss appropriate product release criteria for early clinical studies.

ATMP process development should include a cellular starting material stability study to justify storage conditions and hold-time between cell collection and ATMP manufacturing[12]. In this study, 19-FiCART manufacturing was initiated from fresh LPs without an intermediate cryopreservation step, which is commonly applied in current commercial CAR T-cell products for logistical reasons[8]. LPs obtained from healthy donors remained stable for 49 h at RT and 73 h at CT, beyond which statistically significant changes were observed in cell composition and cell viability. In the starting material stability study performed for the commercial CAR T-cell product Tisagenlecleucel[19], cells in LPs remained viable for 72 h at 2–8 °C, and cell viability

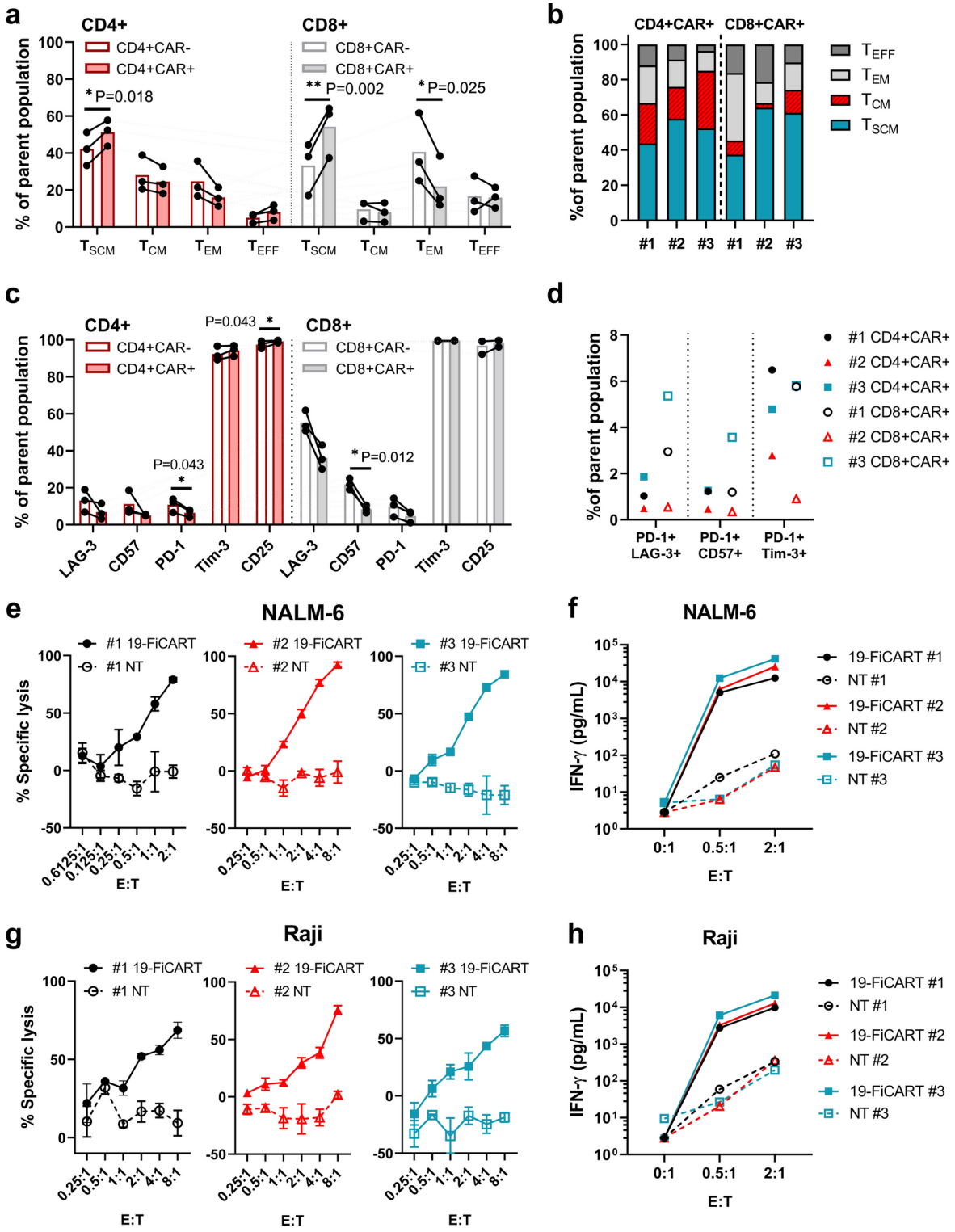

decreased substantially faster at RT than at CT. These data suggest that LPs should be stored at CT to ensure a higher probability of successful manufacturing. While patient-derived LPs may exhibit higher variation in the cell composition[20,21], our data indicate that fresh LPs stored at CT for up to 73 h could be adequate for manufacturing CAR T-cells or other ATMPs. The three-day stability of LPs would enable the use of fresh starting material for local manufacturing or transport over short to medium distances, reducing costs and simplifying the manufacturing process and logistics by eliminating cell freezing and ultra-low temperature transport steps. It should be noted, however, that the current study did not include the production of CAR T-cells from LPs stored under the tested conditions. Therefore, additional studies evaluating the identity and potency of CAR T-cells produced from LPs stored at CT for 73 h are necessary to confirm that these conditions are adequate for storing LPs prior to CAR T-cell manufacturing.

◀**Fig. 4**. 19-FiCART product T-cell phenotype and performance in in vitro potency assays. The phenotype of CAR-positive and CAR-negative CD4+ and CD8+ cells in day 12 DS products was assessed by flow cytometry. **a**) Frequencies of T-cell memory phenotype subsets (T_{SCM}, T_{CM}, T_{EM}, and T_{EFF}) in CAR+ and CAR-CD4+ and CD8+ cells. **b**) Frequencies of T-cell memory phenotype subsets in the CD4+CAR+ and CD8+CAR+ populations shown for individual process runs (#1–3). **c**) Frequencies of cells expressing T-cell exhaustion markers (LAG-3, CD57, PD-1, Tim-3) and CD25 within CAR+ and CAR-CD4+ and CD8+ cells. **d**) Frequencies of cells co-expressing PD-1 with LAG-3, CD57, or Tim-3 in the CD4+CAR+ and CD8+CAR+ populations shown for individual process runs (#1–3). **e**–**h**) The in vitro anti-tumor activity of 19-FiCART cells in response to CD19+ RedFluc+ target cell lines, NALM-6 and Raji, shown as % specific lysis of target cells (**e**, **g**) and IFN-γ secretion to culture supernatant (**f**, **h**) during a 20-h co-culture at indicated E:Ts as measured by luciferase assay and IFN-γ ELISA, respectively. **a**, **c**) Data are shown as mean (bars) with individual data points for individual process runs (#1–3) with a connecting line between the CAR+ and CAR- cells from the same samples. **e**–**f**) Data are shown for individual process runs (#1–3) as mean ± SD of three replicate co-cultures in cytotoxicity assay (**e**, **g**) and mean of two replicate co-cultures in IFN-γ secretion assay (**f**, **h**). **a**, **c**) Paired t-test (*P < 0.05; **P < 0.01). DS, drug substance; T_{SCM}, stem cell memory T cell; T_{CM}, central memory T cell; T_{EM}, effector memory T cell; T_{EFF}, effector T cell; E:T, effector-to-target cell ratio; IFN-γ, interferon-γ.

Attribute	Parameter (sample)	Analytical method	19-FiCART #1	19-FiCART #2	19-FiCART #3	[a]Planned acceptance criteria
Appearance	Appearance (DS)	visual inspection	opaque, yellowish cell suspension	opaque, yellowish cell suspension	opaque, yellowish cell suspension	opaque, yellowish cell suspension
Purity	%CD3+ T cells (DS)	FCM (%CD45+CD3+CD56- cells)	93.8	95.4	92.8	≥ 80%
Impurity (product related)	%B cells (DS)	FCM (%CD45+CD19+ cells)	0.007	< 0.005	< 0.005	< 2%
	%HSCs (DS)	FCM (%CD45+CD34+ cells)	< 0.005	< 0.005	< 0.005	< 2%
Identity / Potency	Transduction efficiency, %CAR+ T cells (DS)	FCM (%CD45+CD3+CD56-CAR+ cells)	45.7	50.0	72.8	≥ 20%
Potency	%Viability (DS)	PI-based measurement of total and dead nucleated cells (Automated cell counter)	97.2	96.9	97.7	≥ 70%
Potency / Safety	Vector copy number (DS)	ddPCR (vector copies / genome)	1.20	1.16	2.52	< 5 copies
Quantity	Total number of viable cells (DS)	PI-based measurement of total and dead nucleated cells (Automated cell counter)	2.08×10^9	2.33×10^9	3.74×10^9	[b]target yield $\geq 3 \times 10^8$ CAR+CD3+ T cells
	Transduction efficiency (DS)	FCM (%CD45+CD3+CD56-CAR+ cells)				
Safety	Sterility (d0 leukapheresis, [c]d7 IPC, and DP)	Microbial culture assay Ph.Eur. 2.6.27	No growth	No growth	No growth	No growth
	Endotoxin (DP)	Chromogenic LAL method Ph.Eur. 2.6.14	N/A	N/A	N/A	< 5 EU/kg of patient body weight
	Mycoplasma (DP)	ddPCR Ph.Eur.2.6.7 Ph.Eur.2.6.21	N/A	N/A	N/A	Absent

Table 2. Planned early-phase batch release criteria of 19-FiCART with results for development batches #1–3 produced from healthy donor starting material. [a]The planned acceptance criteria are based on published literature[33–36,39,40,42,43,45] and 19-FiCART batch #1–3 results. [b]The target yield of CAR+ T cells is based on a reference dose of 2×10^6 CAR+ T cells/kg (used for Axicabtagene ciloleucel and Brexucabtagene autoleucel[46]) for a 75 kg patient and the material needed for analytical testing (a total of 1.5×10^8 CAR+ T cells for both the dose and the analytics). [c]Sterility testing of d7 IPC was performed only for 19-FiCART batch #1. FCM, flow cytometry; HSC, hematopoietic stem cell; CAR, chimeric antigen receptor; PI, propidium iodide; ddPCR, droplet digital polymerase chain reaction; IPC, in-process control; DS, drug substance; DP, drug product; Ph.Eur., European Pharmacopoiea; LAL, Limulus Amebocyte Lysate; EU, endotoxin unit.

The results of CD4/CD8-enrichement and 19-FiCART product cell composition align with other studies that have produced CAR T-cells using a Prodigy -based protocol that involves CD3/CD28-stimulation, interleukin (IL)-7/15-driven expansion, and LVV transduction[10,22–24]. Post-enrichment recovery (mean 61%) and purity (mean 89%) of CD4/CD8-cells are comparable to previous studies reporting 55–68% recovery[10,22] and 89–98% purity[10,22,23] of CD4/CD8-cells. Similarly, the observed T-cell expansion rates (approximately 50-fold), CD3+ T-cell purity (mean 94%), CD4:CD8 cell ratio (mean 1.8), and NKT-cell impurity (mean 5%), align with previous research on CAR T-cell generation CAR T-cells from healthy donor or patient material[22–24]. The transduction efficiency of CD4+ cells was slightly higher compared to CD8+ cells, consistent with findings from prior studies[10,22–24]. The NKT-cell population in the 19-FiCART products also contained a proportion of CAR+ cells (22–33%), similar to data reported by Blaeschke et al.[24] A more precise definition of NKT cells includes major histocompatibility complex-like molecule CD1d-restricted antigen recognition, rather than co-

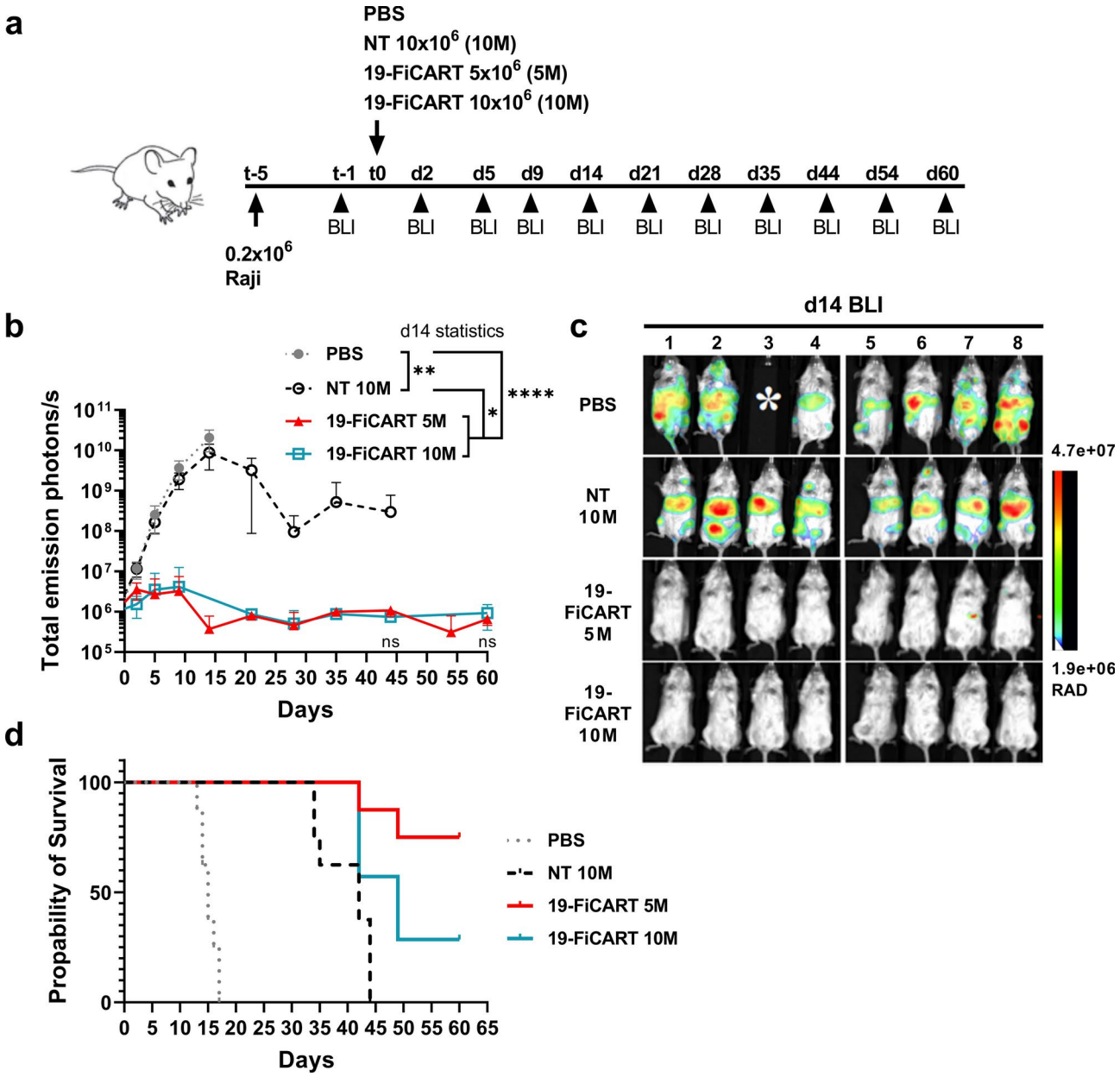

Fig. 5. An in vivo anti-tumor response and survival study. **a**) Experiment outline. **b**) Anti-tumor response of 19-FiCART cells in NSG mice implanted i.v. with 0.2×10^6 Raji-RedFLuc-GFP cells. BLI signal kinetics in the mice treated with PBS, NT, and 19-FiCART cells at the indicated doses. Data are shown as mean ± SD (n = 8). The datapoint for 19-FiCART 10 M group at d14 equals 0 photons/s (signal below detection limit) and is not displayed on the logarithmic scale plot. One-way ANOVA with Tukey's multiple comparison tests between PBS, NT 10 M, 19-FiCART 5 M and 10 M groups at the indicated time points. $P < 0.05$ was considered statistically significant (ns, not significant). ****P = 0.0001 (19-FiCART 5 M/10 M vs PBS). **P = 0.004 (PBS vs NT 10 M). *P = 0.04 (19-FiCART 5 M/10 M vs NT 10 M). **c**) Day 14 representative BLI images of mice treated with PBS, NT 10 M, and 19-FiCART at 5 M and 10 M doses. Mice id: 1–8. The white asterisk indicates a mouse sacrificed due to toxicities. **d**) Probability of survival for the specified groups after 60-day treatment. NSG, nod-scid-gamma; BLI, bioluminescence; PBS, phosphate-buffered saline; NT, non-transduced T cell; M, 1×10^6.

expression of T and NK cell markers[25]. Consequently, it remains uncertain whether the CD3+CD56+ cells in the 19-FiCART products represent true NKT cells or T cells undergoing terminal differentiation, which can express CD56[26].

Less differentiated T-cell phenotypes are desired in adoptive T-cell therapy products due to their high potential for proliferation and persistence *in vivo*[27]. As demonstrated in earlier reports[24,28], the IL-7/15-driven Prodigy TCT protocol induced the generation of less differentiated T-cell memory phenotypes (T_{SCM} and T_{CM}) during culture. Importantly, the CAR+ cells within the CD4+ and CD8+ cells in the 19-FiCART products had slightly less differentiated T-cell memory phenotypes and showed lower expression levels of T-cell exhaustion

markers than the corresponding CAR-negative populations. These results confirm that FiCAR expression did not promote T-cell differentiation towards effector phenotypes, aligning with our previous finding that FiCAR constructs incorporating the CD19-targeting FMC63-scFv are not prone to significant tonic signaling[29].

Similar results were previously reported by Castella et al., who used the Prodigy TCT process to manufacture 28 batches of the autologous CD19-targeted CAR T-cell product (ARI-0001) in a phase I trial for B-cell malignancies[30]. They observed an increase in T_{CM} cells and a decrease in effector T cells within the CAR+ population compared to the CAR-negative population in the ARI-0001 products, although these differences were not statistically significant[30]. This observation was attributed to the 4-1BB costimulatory domain of the CAR, as 4-1BB stimulation has been suggested to increase the expression of the lymphoid homing receptor CCR7, a marker for a less differentiated memory phenotype, in CAR T-cells[31]. In small-scale experiments, they observed that expression of the 4-1BB-based CAR led to marginally increased CCR7 expression in CAR+ cells compared to CAR-negative cells[30]. A similar, though minor, effect was seen when the costimulatory domain was switched to CD28[30]. Given the small number of 19-FiCART batches produced in this study (n = 3), additional data are needed to determine whether expression of the CD28-based FiCAR consistently causes a less differentiated phenotype in CAR+ cells compared to CAR-negative cells within 19-FiCART products. This provides an intriguing question for exploration in future studies.

The 19-FiCART QC plan was designed to address common CAR T-cell product CQAs, including safety, potency, identity, purity, impurities, and quantity[11,32]. The planned batch release tests for early clinical development (Table 2) include tests for appearance, purity (CD3+ T cells), impurities (%CD19+ cells and %CD34+ cells), identity (%CAR+CD3+ T cells), potency (viability, %CAR+ CD3+ T cells, and VCN), quantity (total number of viable CAR+CD3+ T cells), and safety (VCN, sterility, endotoxin, and mycoplasma). Previous publications describing release testing of CAR T-cell products during early-phase development have used essentially similar release tests with variations such as including a potency assay[33], a test for adventitious agents[33], or replication-competent lentivirus/retrovirus (RCL/RCR) tests[33–36]. Additional 19-FiCART batch characterization includes T-cell phenotype analysis and the potency assays measuring cytotoxicity and IFN-γ secretion in response to CD19+ target cells. One of the two potency assays could be chosen for use as part of DP batch release in later phase of development. During early development of 19-FiCART, further product characterization studies could assess various aspects such as residual cytokines and HIV-1 p24 protein, adventitious agents, tumorigenicity, vector integration profile, and RCL[37]. Analytical method validation can follow a phase-appropriate approach, where safety-related tests are validated before entering clinical studies and other methods are validated during early clinical development[38]. A validated potency assay is expected for pivotal trials[38].

Safety testing includes analyses measuring microbial safety, certain cellular impurities, and vector-related safety. During 19-FiCART manufacturing, we assessed the presence of CD34+ HSCs at the beginning and the end of the process, considering the potential for insertional oncogenesis in stem cells. Notably, the small CD34+ population observed in the LPs was effectively removed by CD4/CD8-enrichment and completely absent in the DS products. However, it is essential to verify this finding with patient-derived 19-FiCART batches because the number of CD34+ cells could be different in LPs from patients[39]. When manufacturing autologous CAR T-cells for B-cell malignancies, it is crucial to test for the presence of B cells[32,34,40]. This helps reduce the risk of infusing the patient with transduced blasts. CAR+ blasts could be resistant to CAR T-cell therapy due to CAR expression-mediated masking of the CD19-epitope, potentially increasing the risk of relapse[41]. In the 19-FiCART QC plan, the DS is currently analyzed for CD19+ cells. However, considering CD19-independent detection of B-cells, the assessed B-cell antigen could be switched to CD20. Tentative acceptance criteria for cellular impurities in the DS product could be set at ≤ 2%[40], for example, for early clinical studies and adjusted according to patient material manufacturing data.

In CAR T-cell products, VCN serves as a critical indicator of both safety and potency[37]. While an unofficial FDA recommendation suggests allowing less than five vector copies/genome[42,43], regulatory guidelines emphasize the need to justify VCN acceptance criteria based on process development data[37,44]. To strike a balance between functionality and safety, transduction efficiency should be optimized while minimizing VCN[37,44]. Previous publications on early-phase development of CAR T-cell products have acceptance limits of ≤ 4[34], ≤ 5[36], or ≤ 10[33] copies/cell for VCN, and ≥ 10%[34,36] or 20%[33] for %CAR + cells[33,34]. In the case of 19-FiCART, utilizing three MOIs – 0.3, 0.8, and 1.5 – resulted in approximately 50–80% transduction efficiency and 1.2–2.5 mean VCN per cell. All the three products demonstrated active in vitro cytotoxicity and IFN-γ secretion responses against CD19 + cell lines. Considering the high cost of GMP-quality vector materials, an MOI of 0.3–0.8 would be feasible to ensure the production of functional 19-FiCART cells while maintaining low VCN using the 19-FiCAR LVV. Tentative acceptance limits of transduction efficiency and VCN could be set at ≥ 20% CAR+ T cells and < 5 copies per cell, respectively, and adjusted based on additional data generated during later development.

Adequate viability, purity, and quantity of CAR T-cells are critical for ensuring sufficient therapeutic cells for clinical use. Typically, acceptance limits for cell viability in CAR T products range from ≥ 70% to ≥ 80%[33,34,36,39,40]. For example, Tisagenlecleucel demonstrated a favorable clinical outcome with a cell viability of ≥ 70%[45]. Early-phase CAR T development studies have employed acceptance limits of ≥ 70%[33] , ≥ 80%[36] and ≥ 95%[34] acceptance limits for CD3+ cell purity. Based on these findings and our data, it would be appropriate to establish tentative acceptance criteria of ≥ 80% for CD3+ T-cell purity and ≥ 70% for viability during the early development of 19-FiCART.

To put this into context, a total number of 3×10^8 total CAR+ T cells would allow the treatment of a 75 kg patient with a dose of 2×10^6 CAR + T cells/kg (similar to commercial products Axicabtagene ciloleucel and Brexucabtagene autoleucel[46]). Additionally, this would provide 0.15×10^8 CAR+ T cells for analytical procedures. Notably, a yield of 3×10^8 CAR + T cells was achieved already by d7, suggesting that the twelve-day culture time may be excessively long. During early development, extra material is necessary for stability studies, analytical method validation, and product characterization. The use of a shorter culture time for clinical 19-FiCART

batches is supported by the association between short expansion (3 or 5 days) and higher proportion of less differentiated T cells[47]. As we explore shorter expansion periods, it is crucial to repeat expansion rates and safety-related test using patient-derived 19-FiCART cells before considering culture time reduction.

In addition to VCN, vector-related safety tests encompass the analysis of vector-related impurities and testing for RCL. Testing for RCL is not necessarily required at CAR-T cell batch release if RCL is tested at the level of the vector starting material and a risk assessment addressing the potential RCL formation during manufacturing is presented[37]. Therefore, we planned RCL testing as part of the 19-FiCAR LVV batch release.

Another critical aspect of vector-related safety is the remaining replication-defective infectious vector particles in the final product. For products containing genetically modified cells, an environmental risk assessment is essential to ensure safe handling and clinical use[37,38]. This assessment can be based on a calculating residual replication-defective infectious viral particles in the cell product[48,49]. Alternatively, measuring residual HIV-1 capsid protein p24 in the product supernatant is informative. However, p24 can be present as vector-associated or free protein. Therefore, the detection p24 does not directly indicate the presence of functional LVV particles; it merely reveals the presence of unwanted vector-derived impurity. To our knowledge, the presence of LVV-derived p24 protein impurity in CAR T-cell products manufactured by the Prodigy has not been previously published. Our results demonstrate detectable p24 in the DS supernatant, emphasizing the importance of post-transduction washes during manufacturing. However, we excluded p24 ELISA from the planned batch release test through a risk assessment based on dilution-based calculations of residual infectious particles.

The selection of sampling points (leukapheresis material, IPCs, DS, and DP) and analytical methods used in the QC plan was based on regulatory requirements and practical considerations. For instance, microbial sterility assessment was performed on d7 IPC to enable process termination before d12 in case of positive results, ensuring cost-efficiency during process development. In a clinical setting, negative sterility result for IPC could allow for DP batch release of a fresh CAR T product. We also evaluated the feasibility of using pre-harvest transduction efficiency results on d12 IPC to calculate DP doses during the harvest procedure, thus avoiding delays caused by waiting for post-harvest/DS FCM results. Notably, no significant differences were observed in T-cell composition or CAR + CD3 + T cell frequency between d12 IPC and DS of 19-FiCART batch #1, making it feasible to use pre-harvest transduction efficiency results for DP dose calculations to improve process robustness.

The 19-FiCART cells demonstrated remarkable anti-tumor activity in our Raji cell CD19+ lymphoma mouse model at both 10 M and 5 M doses. However, in contrast to 10 M NT and 19-FiCART, 5 M 19-FiCART cell dose effectively cleared the tumor load in the treated mice with a noticeably reduced incidence of severe adverse events (100% vs 75% vs 25% mice toxicities in 10 M NT, 10 M 19-FiCART and 5 M 19-FiCART, respectively). The tumor-bearing PBS-treated mice developed hindlimb paralysis likely due to metastasis of Raji cells to the nervous system[50]. In contrast, NT and 19-FiCART cell-treated mice manifested toxicities likely resulting from GvHD—a disorder commonly associated with allogeneic cell transplantation but does not occur in autologous settings. The severity of the toxicities in CAR T-cell therapies is associated, among others, with the potency and dose[51]. Strategies to prevent and/or manage CAR T-cell associated toxicities include low doses or using a split CAR design[52,53]. In this line, our results demonstrate an effective and much safer anti-tumor response by the 19-FiCART cells when used at the low (5 M) dose; however, further preclinical toxicity testing with a 5 M NT cell dose and an additional number of 19-FiCART batches is still required to fully corroborate the efficacy and safety in an in vivo model.

This study successfully established a platform for manufacturing and analytically testing of functionally potent 19-FiCART cells. This paper provides insights into early development of CAR T-cell products and other ATMPs produced using LPs as the starting material. The FiCAR construct's retargetability against different antigens by switching the antigen-recognizing structure enables targeting of different antigens with FiCAR T-cells in the future.

Materials and methods

Leukapheresis collection and stability study

Non-mobilized LPs were collected at the Finnish Red Cross Blood Service (FRCBS) in Helsinki, Finland from healthy, voluntary donors. Written informed consent was obtained and handling followed a study plan approved by the Ethics Committee, Hospital District of Helsinki and Uusimaa (HUS/289/2022). The study was conducted in accordance with the ethical guidelines of the Declaration of Helsinki. Testing donors for infective agents adhered to requirements for donors of autologous starting material (EU directive 2006/17/EC). Apheresis utilized the Spectra Optia continuous mononuclear cell protocol (Version 11, Terumo BCT, Lakewood, CO). The LPs were stored at RT until further processing on the same day.

For stability evaluation, remaining LP materials not used for (19-FiCART) manufacturing were divided into two parallel collection bags and stored at 15–25 °C (RT) and 2–8 °C (CT). We assessed product stability at five time points (T0, 25 h, 49 h, 73 h, 121 h) by visual inspection of appearance, measurement of WBC count (Sysmex pocH 100i analyzer, Sysmex, Kobe, Japan), and flow cytometry (FCM) analysis of leukocyte composition, viability, and apoptotic cells. Detailed method descriptions are provided in the flow cytometry subsection.

CAR construct and lentiviral vectors

The CAR used (mod FiCAR 1) is a modified form of the construct previously described as FiCAR 1 in our earlier publication[13]. Briefly, the FiCAR 1 comprises a CD19-targeted extracellular FMC63 domain connected via an extended human IgG1-derived hinge and a linker to a spacer structure composed of two SIRPα-derived Ig-like domains. The FiCAR 1 transmembrane and co-stimulatory domains are formed from human CD28 and the signaling domain from human T cell receptor CD3ζ.-chain. In the modFiCAR 1 construct, the extended IgG1-hinge of the FiCAR 1 is replaced with a human IgG4-hinge (UniProt sequence id: P01861), modified for functionality[54,55].

Vesicular stomatitis virus-G protein pseudotyped, 3rd generation self-inactivating LVVs encoding modFiCAR 1 were produced by a GMP-competent CDMO (VIVEbiotech, Spain). The LVVs were formulated in TexMACS GMP Medium (Miltenyi Biotec, Bergisch Gladbach, Germany) and stored at -80 °C. In each 19-FiCART batch (#1–3, see below) a vector from a separate LVV production batch was used. The LVVs were provided with a quantitative polymerase chain reaction titer of virus determined in HEK293T cells. For LVVs from processes #1 and #3, we determined the primary T-cell LVV-titer (see vector copy number analysis for details), which was approximately three times higher than the provided HEK293T titer (data not shown). The HEK293T titer was used for calculating the MOI in the 19-FiCART manufacturing process.

19-FiCART manufacturing process and planned QC strategy

Three batches of 19-FiCART (#1–3) were manufactured using the CliniMACS Prodigy equipped with the TS520 tubing set and the TCT software v2.0.10[10] (all from Miltenyi Biotec). Manufacturing was performed in a biosafety level 2-classified grade D clean room. Open process steps, including reagent preparations, DS sampling, final formulation, and DP filling, were performed in a grade A Bioquell QUBE isolator (Bioquell Ltd., Andover, UK). The process buffer, CliniMACS phosphate-buffered saline (PBS)/ethylene-diamine-tetraacetic acid (EDTA) Buffer (Miltenyi Biotec) supplemented with 2% v/v Albunorm 200 g/l (Octapharma AB, Stockholm, Sweden), and the culture medium, TexMACS GMP Medium supplemented with 12.5 ng/mL MACS GMP Recombinant Human IL-7 and IL-15 (all from Miltenyi Biotec), were prepared before starting the process. The 19-FiCART manufacturing process flow chart and planned QC strategy are depicted in Fig. 2.

On d0, CD4/CD8-cell count in the LP material was determined based on WBC count (Sysmex pocH 100i analyzer, Sysmex, Kobe, Japan) and the frequency of CD4/CD8-labeled cells assessed by FCM. CD4+ and CD8+ cell enrichment was performed with the Prodigy using $1–3 \times 10^9$ CD4/CD8+ cells and the CliniMACS CD4 and CD8 Reagents (Miltenyi Biotec). Subsequently, 10^8 CD4/CD8-enriched cells were activated with a 1:17.5 ratio of MACS GMP T Cell TransAct (Miltenyi Biotec) reagent for 16 (+/- 1) hours at + 37 °C, 5% CO_2 in 70 mL total volume. Additionally, 10^6 CD4/CD8-enriched cells were used to produce NT control cells for reference in analytical tests (Supplementary Table S3).

Transduction was performed on d1 by adding the LVV and culture medium (30 mL) to the cell culture, resulting in a 100 mL total volume. The LVV was used at varying MOIs in processes #1–3 (0.3, 0.8, and 1.5, respectively). Cells were cultured for twelve days, during which two culture washes were performed (on d3 and d5), the culture volume was increased to 250 mL, and daily medium exchanges were performed (see Supplementary Table S3). On d12, the DS product was harvested in 100 mL of Natriumklorid Baxter Viaflo 9 mg/ml solution (Baxter S.A, Lessines, Belgium) containing 23.6% v/v Albunorm 200 g/l. For final formulation, 5% v/v dimethyl sulfoxide (CryoSure-DMSO, WAK-Chemie Medical GmbH, Steinbach/Ts, Germany) was added to the DS to form the DP (Fig. 2). The DP was frozen with a BIOFREEZE Smartline controlled rate freezer (Consarctic GmbH, Westerngrund, Germany) and transferred to a vapor phase liquid nitrogen freezer.

The 19-FiCART QC plan was designed based on the EMA guidelines EMA/523,923/2020[37] and EMEA/CHMP/410,869/2006[12], as well as the Guidelines on Good Manufacturing Practice specific to Advanced Therapy Medicinal Products[38], and the European Pharmacopoeia. The analytics performed on the LP starting materials, IPCs, DS, and DP are described in Fig. 2. Appearance was assessed by visual inspection and microbial sterility using BACT/ALERT VIRTUO (BioMérieux, Étoile, France) with aerobic (FA Plus or BPA) and anaerobic (FN Plus) culture bottles (BioMérieux). Cell count and viability were measured by the NucleoCounter NC-100 cell counter (ChemoMetec, A/S, Allerod, Denmark). Leukocyte composition, transduction efficiency, and T-cell phenotype were analyzed by FCM. Potency was assessed by cytotoxicity and IFN-γ secretion assays, VCN by droplet digital PCR (ddPCR), and HIV-1 p24 protein impurity by p24 ELISA. Data are not available for the endotoxin and mycoplasma tests.

Flow cytometry

We used FCM analyses to assess product cell composition, transduction efficiency, and T-cell phenotype at various time points during the 19-FiCART manufacturing process (Fig. 2 and Table 3). The marker expression patterns and cell type definitions in each analysis are shown in Supplementary Table S4. In the LP stability study, leukocyte composition was analyzed using the same analytical method as for LP material in 19-FiCART production (Table 3). For cell apoptosis analysis, cells were stained with a mixture of anti-human antibodies against CD45, CD56, CD4, CD8, and CD3, 7-aminoactinomycin D (7-AAD) viability stain, and Apotracker Green (APO-15). The antibodies and viability stains used in the analyses are listed in Supplementary Table S5 and specific antibody panels are shown in Supplementary Tables S6–S10. The FCM buffer consisted of PBS (Cell Therapy Systems, DPBS CTS Dulbecco's PBS, Gibco) containing 0.5% HSA (Albunorm, Octapharma) and 2 mM EDTA (Ultrapure EDTA, Gibco, Life technologies, Grand Island, NY). Red blood cells were lysed from the LP samples using a Red Blood Cell Lysis Solution (Miltenyi Biotec). Cells were incubated with antibodies at a density of 10^6 cells/100 µl for 15 min at RT. All post-transduction samples were fixed with 1% paraformaldehyde in PBS (Thermo Fisher Scientific, Fair Lawn, NJ) for 30 min at 4 °C before analysis (Table 3).

FCM was performed using the DxFLEX flow cytometer (Beckman Coulter Life Sciences, Brea, CA). The analysis of leukocyte composition, transduction efficiency, and cellular impurities were performed in duplicate for the samples indicated in Table 3. Other analyses were performed in single tubes. The number of stained cells and acquired events in each analysis are shown in Table 3. Appropriate isotype controls or fluorescence minus one controls were used for gating cell type-specific markers and NT cells served as gating reference for CAR+ cells. Veri-Cells CD34 PBMC (Biolegend) was used as a control for gating CD34+ cells. Gating strategies for the 19-FiCART QC analyses are shown in Supplementary Fig. S7–S9. Additionally, gating strategies for analyzing cell type-specific viability and apoptosis in the LP stability study are presented in Supplementary Fig.

Day (d)	Analysis name	Sample	Markers	Number of cells stained / Number of events acquired in FCM (live cells)
d0	Leukocyte composition	[a, b]LP	CD3; CD4; CD8; CD14; CD19; CD45; CD56; 7-AAD	1×10^6 / 5×10^4
		d0 IPC (CD4/CD8-enrichment positive fraction)		
		CD4/CD8-enrichment negative fraction		
	CD34 + cells	LP	CD34; CD45; 7-AAD	2×10^6 /1×10^6
		d0 IPC (CD4/CD8-enrichment positive fraction)		
d7, d12	[c]Transduction efficiency	d7 IPC	CD3; CD4; CD8; CD19; CD45; CD56; CD19-CAR FMC63; Zombie Aqua	1×10^6 / 5×10^4
		[d]d12 IPC (before harvest)		
		[b]DS		
d12	[c]Cellular impurities	[b]DS	CD14; CD19; CD34; CD45; Zombie Aqua	2×10^6 / 1×10^6
	[c]T-cell memory phenotype	DS	CD4; CD8; CD19 CAR FMC63; CCR7; CD45RA; CD45RO; CD95; Zombie Aqua	1×10^6 / 1×10^5
	[c]T-cell activation and exhaustion	DS	CD4; CD8; CD19 CAR FMC63; LAG-3; CD57; Tim-3; PD-1; CD25; Zombie Aqua	1×10^6 / 1×10^5

Table 3. Flow cytometry analyses, samples, and markers utilized to assess the cellular composition, transduction efficiency, and T-cell phenotype at different time points during the 19-FiCART production process. [a]The frequency of CD4/CD8-labeled cells in the LP material entered to the CliniMACS Prodigy before the CD4/CD8-enrichment was gated on total cells without dead cell discrimination based on 7-AAD positivity. [b]Staining and analysis in duplicates. [d]Day 12 IPC was analyzed only in process #1. FCM, flow cytometry; LP, leukapheresis product; CAR, chimeric antigen receptor; IPC, in-process control; DS, drug substance; T_N, naïve T cell; T_{SCM}, stem cell memory T cell; T_{CM}, central memory T cell; T_{EM}, effector memory T cell; T_{EFF}, effector T cells; PD-1, programmed death 1; LAG-3, lymphocyte-activation gene 3; Tim-3, T cell immunoglobulin and mucin domain-containing protein 3.

S10 and Fig. 1c, respectively. Data analyses were performed using FlowJo software (Version 10.0.7r2, FlowJo LLC, Ashland, OR).

Cell lines

To create *Luciola italica* luciferase (RedFLuc) and Green Fluorescent Protein (GFP)-expressing target cells for the potency assays, CD19+ B-lineage acute lymphocytic leukemia cells (NALM-6 cell line; purchased from American Type Culture Collection, ATCC, Manassas, VA, USA, cat. CRL-3273), and Burkitt's lymphoma cells, (Raji cell line; purchased from ATCC, cat. CCL-86), were transduced using IVISbrite Red F-luc-GFP Lentiviral Particles (RediFect, Perkin Elmer, Boston, MA). The GFP+ cells were purified using the Sony SH800 cell sorter (Sony Biotechnology, San Jose, United States). Cell lines were cultured in RPMI-1640 medium supplemented with 10% Fetal Bovine Serum (FBS) and 100 IU/mL penicillin–streptomycin (all from Gibco). Cell cultures were maintained at 37 °C 5% CO_2.

Potency assays

Potency was evaluated by measuring in vitro cytotoxicity and IFN-γ secretion by 19-FiCART cells in response to CD19+ target cells. In the assays, 19-FiCART cells were incubated for 20 h at 37 °C, 5% CO_2 with NALM-6-RedLuc-GFP or Raji-RedLuc-GFP target cells in RPMI-1640 medium containing 10% FBS and 100 U/mL penicillin–streptomycin. The number of plated 19-FiCART cells was determined using the number of live CAR + T-cells and the number of target cells based on the number of live cells. The cytotoxicity assay was performed in 96-well plates using several E:T ratios (range 0.0625–8:1). For bioluminescence detection, cells were lysed with the neolite Reporter Gene Assay System reagent (Perkin Elmer), and the results were measured using the Victor Nivo F3 plate reader (Perkin Elmer). Specific lysis of target cells was calculated using the luminescence of target cells alone as a control corresponding to 0% killing. The IFN-γ assay was performed in 48-well plates using E:T ratios of 0.5:1 and 2:1. The culture supernatants were collected and stored at -70 °C until IFN-γ quantification by the Human IFN-gamma Quantikine ELISA Kit (R&D Systems, Minneapolis, MN).

Vector copy number analysis and p24 ELISA

The absolute number of integrated vector copies per cell in 19-FiCART cells was determined using the QX200 ddPCR system (Bio-Rad Laboratories, Hercules, CA, USA). Genomic DNA was extracted from 10^6 cells using the EZ1&2 DNA Tissue Kit for automated purification of DNA from cultured cells and the EZ2 Connect instrument according to manufacturer's protocol (Qiagen, Hilden, Germany). DNA concentration was measured by the DeNovix DS-11 FX Spectrophotometer (DeNovix, Wilmington, USA). The ddPCR assay was performed using the ddPCR Multiplex Supermix and expert design probes for detecting the vector sequence (HivPsi in FAM, assay ID: dEXD14812826) along with a housekeeping gene (RPP30 in HEX, assay ID: dHsaCP2500350) and the compatible restriction enzyme Hae III according to the manufacturer's protocol (Bio-Rad Laboratories, Hercules, CA, USA). Droplets were generated using the QX200 Automated droplet generator and PCR amplification was performed on the C1000 Touch Thermal cycler (Bio-Rad Laboratories, Hercules, CA, USA).

VCN was analyzed using the Auto DG QX200 droplet reader PCR system and QX Manager Standard Edition software (version 1.2.345.0909, https://www.bio-rad.com/en-fi/life-science/digital-pcr/qx-software, Bio-Rad Laboratories, Hercules, CA, USA).

To quantify the amount of residual vector-derived HIV-1 p24 protein in the 19-FiCART product, we measured the concentration of p24 in the DS supernatant using the One Wash Lentivirus Titer Kit (Origene, Rockville, MD), and the EnSPire Multimode Platereader (PerkinElmer).

In vivo study

Female NOD.Cg-Prkdcscid Il2rgtm1Wjl/SzJ (NOD-scid-gamma; NSG) mice (4–5 weeks old) were purchased from the Jackson Laboratory (Scanbur, Denmark). Raji-RedFLuc-GFP cells (0.2×10^6 in 100 µL PBS) were injected via the tail vein into the mice and grown for five days. The mice were randomized based on similar tumor load per mouse into four groups (n = 8/group). The NT and 19-FiCART cells from the production batch #3 were thawed in a + 37 °C water bath, formulated in PBS, and injected to the mice (d0) via the tail vein in a 100 µl volume. The 19-FiCART cells were administered at doses of 5×10^6 and 10×10^6 CAR T-cells (hereinafter referred to as 5 M and 10 M). The 19-FiCART doses were calculated based on the transduction efficiency, and cell viability after thawing and passing the cell solution through a 30G needle (BD). Total number of T cells administered in each group are detailed in Supplementary Fig. S5A. In the 10 M NT group, mice received an equal number of total T cells as was given to 10 M 19-FiCART group (Supplementary Fig. S5A). Tumor progression was monitored by non-invasive in vivo bioluminescence imaging (BLI) with CoA D-luciferin sodium salt substrate (#bc218, Synchem, Germany) injected intraperitoneally at 150 mg/kg. BLI images were acquired 10 min after D-luciferin injection with the SPECTRAL Lago X Imaging System under isoflurane (1000 mg/g Attane vet; Piramal Critical Care B.V, Netherlands) anesthesia and analyzed with Aura Imaging Software v4.0.0 (Spectral Instruments Imaging; USA). The mice were monitored at regular intervals for behavior, activity, feeding, and weight. At the end of the experiment, mice were euthanized with a lethal dose of ketamine-xylazine (#511,485, Intervet; #148,999, Orion Pharma). Animal experiments were approved by the Finnish National Animal Experiment Board (License number: ESAVI/10,548/2019) and conducted in accordance with the Finnish Act on the Protection of Animals Used for Scientific or Educational Purposes, and the University of Helsinki guidelines. The study is reported in adherence to ARRIVE guidelines.

Statistical analysis

GraphPad Prism Software versions 7 and 9.0 for Windows (San Diego, CA, USA) were used for statistical analysis and data plotting. To test for the statistical significances of differences between several groups, we employed Friedman's nonparametric ANOVA for repeated measures followed Dunn's post-test for multiple comparisons or one-way ANOVA with Tukey's correction for multiple comparisons. the paired t-test was used for comparisons between paired groups. It is important to note that the assessment of data distribution is impaired due to the small sample size (n = 3–8), and the results of the parametric statistical tests apply only if the data follow normal distribution. The statistical tests used for individual analyses are indicated in the figure legends. A significance level of $P \leq 0.05$ was considered statistically significant. Data are reported as mean ± standard deviation (SD), unless otherwise specified.

Data availability

The data generated in this study are available from the corresponding author upon reasonable request.

Received: 11 October 2024; Accepted: 3 March 2025
Published online: 08 March 2025

References

1. Elsallab, M. & Maus, M. V. Expanding access to CAR T cell therapies through local manufacturing. *Nat. Biotechnol.* **41**, 1698–1708 (2023).
2. Giorgioni, L., Ambrosone, A., Cometa, M. F., Salvati, A. L. & Magrelli, A. CAR-T State of the Art and Future Challenges, A Regulatory Perspective. *Int. J. Mol. Sci.* **24**, 11803 (2023).
3. Wang, V., Gauthier, M., Decot, V., Reppel, L. & Bensoussan, D. Systematic Review on CAR-T Cell Clinical Trials Up to 2022: Academic Center Input. *Cancers (Basel)* **15**, 1003 (2023).
4. Priesner, C. & Hildebrandt, M. Advanced therapy medicinal products and the changing role of Academia. *Transfus. Med. Hemotherapy* **49**, 158–162 (2022).
5. Delgadillo, J. et al. A management model in blood, tissue and cell establishments to ensure rapid and sustainable patient access to advanced therapy medicinal products in Europe. *Cytotherapy* **25**, 1259–1264 (2023).
6. Watanabe, N., Mo, F. & McKenna, M. K. Impact of manufacturing procedures on CAR T cell functionality. *Front. Immunol* **13**, 876339 (2022).
7. Dickinson, M. J. et al. A Novel autologous CAR-T therapy, YTB323, with preserved T-cell stemness shows enhanced CAR T-cell efficacy in preclinical and early clinical development. *Cancer Discov* **13**, 1982–1997 (2023).
8. Levine, B. L., Miskin, J., Wonnacott, K. & Keir, C. Global manufacturing of CAR T cell therapy. *Mol. Ther. Methods Clin. Dev.* **4**, 92–101 (2017).
9. Martinez-Cibrian, N., Español-Rego, M., Pascal, M., Delgado, J. & Ortiz-Maldonado, V. Practical aspects of chimeric antigen receptor T-cell administration: From commercial to point-of-care manufacturing. *Front. Immunol.* **13**, 1005457 (2022).
10. Zhu, F. et al. Closed-system manufacturing of CD19 and dual-targeted CD20/19 chimeric antigen receptor T cells using the CliniMACS Prodigy device at an academic medical center. *Cytotherapy* **20**, 394–406 (2018).
11. Reddy, O. L., Stroncek, D. F. & Panch, S. R. Improving CAR T cell therapy by optimizing critical quality attributes. *Semin Hematol* **57**, 33–38 (2020).
12. European Medicines Agency. GUIDELINE ON HUMAN CELL-BASED MEDICINAL PRODUCTS. EMEA/CHMP/410869/2006. https://www.ema.europa.eu/en/documents/scientific-guideline/guideline-human-cell-based-medicinal-products_en.pdf (2008).

13. Koski, J. et al. Novel modular chimeric antigen receptor spacer for T cells derived from signal regulatory protein alpha Ig-like domains. *Front. Mol. Med.* **2**, 1049580 (2022).
14. Hastings, W. D. et al. TIM-3 is expressed on activated human CD4+ T cells and regulates Th1 and Th17 cytokines. *Eur. J. Immunol.* **39**, 2492–2501 (2009).
15. Sheng, M. K., Vick, L., Collins, C., Yoon, D. J. & Murphy, W. J. Asymmetrical Expression of PD1 and CD25 in T-cells Post-Initial Activation. *J. Immunol.* **210**, 226-18–226-18 (2023).
16. Disis, M. L., Bernhard, H. & Jaffee, E. M. Use of tumour-responsive T cells as cancer treatment. *Lancet* **373**, 673–683 (2009).
17. Falkenburg, J. H. F. & Jedema, I. Graft versus tumor effects and why people relapse. *Hematol. Am Soc Hematol. Educ. Program* **2017**, 693–698 (2017).
18. Ullman-Culleré, M. H. & Foltz, C. J. Body condition scoring: a rapid and accurate method for assessing health status in mice. *Lab Anim Sci* **49**, 319–323 (1999).
19. Tyagarajan, S., Schmitt, D., Acker, C. & Rutjens, E. Autologous cryopreserved leukapheresis cellular material for chimeric antigen receptor–T cell manufacture. *Cytotherapy* **21**, 1198–1205 (2019).
20. Harrer, D. C. et al. Apheresis for chimeric antigen receptor T-cell production in adult lymphoma patients. *Transfusion (Paris)* **62**, 1602–1611 (2022).
21. Qayed, M. et al. Leukapheresis guidance and best practices for optimal chimeric antigen receptor T-cell manufacturing. *Cytotherapy* **24**, 869–878 (2022).
22. Aleksandrova, K. et al. Functionality and Cell Senescence of CD4/ CD8-Selected CD20 CAR T Cells Manufactured Using the Automated CliniMACS Prodigy® Platform. *Transfus. Med. Hemotherapy* **46**, 47–54 (2019).
23. Kretschmann, S. et al. Successful generation of CD19 chimeric antigen receptor (CAR) T cells from patients with advanced Systemic Lupus Erythematosus (SLE). *Transplant. Cell. Ther.* **29**, 27–33 (2023).
24. Blaeschke, F. et al. Induction of a central memory and stem cell memory phenotype in functionally active CD4+ and CD8+ CAR T cells produced in an automated good manufacturing practice system for the treatment of CD19+ acute lymphoblastic leukemia. *Cancer Immunol. Immunotherapy* **67**, 1053–1066 (2018).
25. Courtney, A. N., Tian, G. & Metelitsa, L. S. Natural killer T cells and other innate-like T lymphocytes as emerging platforms for allogeneic cancer cell therapy. *Blood* **141**, 869–876 (2023).
26. Good, C. R. et al. An NK-like CAR T cell transition in CAR T cell dysfunction. *Cell* **184**, 6081-6100.e26 (2021).
27. Gattinoni, L., Speiser, D. E., Lichterfeld, M. & Bonini, C. T memory stem cells in health and disease. *Nat. Med.* **23**, 18–27 (2017).
28. Lock, D. et al. Automated manufacturing of potent CD20-directed chimeric antigen receptor T Cells for clinical use. *Hum. Gene. Ther.* **28**, 914–925 (2017).
29. Jahan, F. et al. Using the Jurkat reporter T cell line for evaluating the functionality of novel chimeric antigen receptors. *Front. Mol. Med.* **3**, 1070384 (2023).
30. Castella, M. et al. Point-Of-Care CAR T-Cell Production (ARI-0001) Using a Closed Semi-automatic Bioreactor: Experience From an Academic Phase I Clinical Trial. *Front Immunol* **11**, 00482 (2020).
31. Kawalekar, O. U. et al. Distinct Signaling of Coreceptors Regulates Specific Metabolism Pathways and Impacts Memory Development in CAR T Cells. *Immunity* **44**, 380–390 (2016).
32. Tyagarajan, S., Spencer, T. & Smith, J. Optimizing CAR-T Cell Manufacturing Processes during Pivotal Clinical Trials. *Mol. Ther. Methods Clin. Dev.* **16**, 136–144 (2020).
33. Castella, M. et al. Development of a Novel Anti-CD19 Chimeric Antigen Receptor: A Paradigm for an Affordable CAR T Cell Production at Academic Institutions. *Mol. Ther. Methods Clin. Dev.* **12**, 134–144 (2019).
34. Hollyman, D. et al. Manufacturing validation of biologically functional T cells targeted to CD19 antigen for autologous adoptive cell therapy. *J. Immunother.* **32**, 169–180 (2009).
35. Gardner, R. A. et al. Intent-to-treat leukemia remission by CD19 CAR T cells of defined formulation and dose in children and young adults. *Blood* **129**, 3322–3331 (2017).
36. Wang, X. et al. Phase 1 studies of central memory-derived CD19 CAR T-cell therapy following autologous HSCT in patients with B-cell NHL. *Blood* **127**, 2980–2990 (2016).
37. European Medicines Agency. Guideline on quality, non-clinical and clinical aspects of medicinal products containing genetically modified cells. EMA/CAT/GTWP/671639/2008 Rev. 1 Corr. https://www.ema.europa.eu/en/documents/scientific-guideline/guideline-quality-non-clinical-and-clinical-aspects-medicinal-products-containing-genetically-modified-cells-revision-1_en.pdf (2020).
38. European Commission & Directorate-General for Health and Food Safety. EudraLex, The Rules Governing Medicinal Products in the European Union, Volume 4, Good Manufacturing Practice, Guidelines on Good Manufacturing Practice specific to Advanced Therapy Medicinal Products. https://health.ec.europa.eu/latest-updates/eudralex-volume-4-eu-guidelines-good-manufacturing-practice-medicinal-products-human-and-veterinary-2022-02-21_en (2017).
39. Roddie, C., O'Reilly, M., Pinto, J. D. A., Vispute, K. & Lowdell, M. Manufacturing chimeric antigen receptor T cells: issues and challenges. *Cytotherapy* **21**, 327–340 (2019).
40. Gee, A. P. Manufacturing genetically modified T cells for clinical trials. *Cancer Gene Ther.* **22**, 67–71 (2015).
41. Ruella, M. et al. Induction of resistance to chimeric antigen receptor T cell therapy by transduction of a single leukemic B cell. *Nat. Med.* **24**, 1499–1503 (2018).
42. Santeramo, I. et al. Vector Copy Distribution at a Single-Cell Level Enhances Analytical Characterization of Gene-Modified Cell Therapies. *Mol. Ther. Methods Clin. Dev.* **17**, 944–956 (2020).
43. Zhao, Y., Stepto, H. & Schneider, C. K. Development of the first world health organization lentiviral vector standard: Toward the production control and standardization of lentivirus-based gene therapy products. *Hum. Gene Ther. Methods* **28**, 205–214 (2017).
44. US Food and Drug Administration. *Considerations for the Development of Chimeric Antigen Receptor (CAR) T Cell Products; Draft Guidance for Industry. FDA-2021-D-0404.* https://www.fda.gov/regulatory-information/search-fda-guidance-documents/considerations-development-chimeric-antigen-receptor-car-t-cell-products (2022).
45. Chong, E. A. et al. CAR T cell viability release testing and clinical outcomes: is there a lower limit?. *Blood* **134**, 1873–1875 (2019).
46. Rotte, A. et al. Dose–response correlation for CAR-T cells: a systematic review of clinical studies. *J. Immunother Cancer* **10**, e005678 (2022).
47. Ghassemi, S. et al. Reducing Ex Vivo Culture Improves the Antileukemic Activity of Chimeric Antigen Receptor (CAR) T Cells. *Cancer Immunol Res* **6**, 1100–1109 (2018).
48. European document. Good practice on the assessment of GMO-related aspects in the context of clinical trials with human cells genetically modified by means of retro/lentiviral vectors. https://health.ec.europa.eu/system/files/2021-11/gmcells_gp_en_0.pdf (2019).
49. COGEM. Inschaling van laboratoriumwerkzaamheden met lentivirale vectoren. COGEM Advies CGM/090331–03. 1–46 https://cogem.net/app/uploads/2019/07/Microsoft-Word-090331-03-Brief-en-Generiek-advies-lentivirale-vectoren.pdf (2009).
50. Zhang, L. et al. Selective killing of Burkitt's lymphoma cells by mBAFF-targeted delivery of PinX1. *Leukemia* **25**, 331–340 (2011).
51. Zhou, X. et al. Toxicities of chimeric antigen receptor t cell therapy in multiple myeloma: An overview of experience from clinical trials, pathophysiology, and management strategies. *Front. Immunol.* **11**, 620312 (2020).
52. Monzo, H. J. et al. Efficacy and safety of glycosphingolipid SSEA-4 targeting CAR-T cells in an ovarian carcinoma model. *Mol. Cancer Ther.* **22**, 1319–1331 (2023).
53. Chen, Y. Y. Increasing T Cell versatility with SUPRA CARs. *Cell* **173**, 1316–1317 (2018).

54. Peters, S. J. et al. Engineering an improved IgG4 molecule with reduced disulfide bond heterogeneity and increased fab domain thermal stability. *J. Biol. Chem.* **287**, 24525–24533 (2012).
55. Li, N. et al. The IgG4 hinge with CD28 transmembrane domain improves VHH-based CAR T cells targeting a membrane-distal epitope of GPC1 in pancreatic cancer. *Nat. Commun.* **14**, 1986 (2023).

Acknowledgements
We express our gratitude to Simona Guidi from ProPharma Group for GMP compliance support. Additionally, we acknowledge Sanna Virtaniemi, Johanna Matikainen, Jenni Toivonen, Lotta Andersson, Leila Taalikainen, and Satu Happonen from the Advanced Cell Therapy Centre of the Finnish Red Cross Blood Service, as well as Mari Rissanen and Nadezhda Zinovkina from the University of Helsinki, for technical assistance. Lastly, we thank the Laboratory Animal Center (LAC) and the Biomedicum Imaging Unit (BIU) at the University of Helsinki for support in animal care and imaging.

Author contributions
Conception and design of the study: A.Lu., A.V., M.P., E.K., A.K., H.H., A.La., J.K., M.K., J.L., T.O., H.P., A.A., A.T., B.V., P.M.O., H.M. Data acquisition: A.Lu., A.V., M.P., E.K., A.K., H.H., J.K., V.N., H.P., M.N., E.E., H.M. Data analysis and interpretation: A.Lu., A.V., M.P., E.K., A.K., H.H., J.K., V.N., H.P., M.N., V.K., E.E., A.A., H.M. Drafting and revising the manuscript: A.Lu., H.H., A.La., H.M., P.M.O. All authors contributed to the manuscript and approved the final version.

Funding
This study was funded by Orion Pharma.

Declarations

Competing interests
J.L., T.O., H.P., A.A., V.N., M.N., E.E., V.K., B.V., and A.T. were employed by Orion Pharma during this project. A.A. is a current employee of MSD Finland. P.M.O. and H.M. have performed CRO work for Orion Pharma in the development of FiCAR-based CAR T-cell therapies. M.K. and J.K. are inventors of a CAR structure-related patent application. The remaining authors have no commercial, proprietary, or financial interest in the products or companies described in this article.

Additional information
Supplementary Information The online version contains supplementary material available at https://doi.org/10.1038/s41598-025-92736-9.

Correspondence and requests for materials should be addressed to A.L.

Reprints and permissions information is available at www.nature.com/reprints.

Publisher's note Springer Nature remains neutral with regard to jurisdictional claims in published maps and institutional affiliations.

Open Access This article is licensed under a Creative Commons Attribution-NonCommercial-NoDerivatives 4.0 International License, which permits any non-commercial use, sharing, distribution and reproduction in any medium or format, as long as you give appropriate credit to the original author(s) and the source, provide a link to the Creative Commons licence, and indicate if you modified the licensed material. You do not have permission under this licence to share adapted material derived from this article or parts of it. The images or other third party material in this article are included in the article's Creative Commons licence, unless indicated otherwise in a credit line to the material. If material is not included in the article's Creative Commons licence and your intended use is not permitted by statutory regulation or exceeds the permitted use, you will need to obtain permission directly from the copyright holder. To view a copy of this licence, visit http://creativecommons.org/licenses/by-nc-nd/4.0/.

© The Author(s) 2025